10-Methylacridine Derivatives Acting as Efficient and Stable Photocatalysts in Reductive Dehalogenation of Halogenated Compounds with Sodium Borohydride via Photoinduced Electron Transfer

Masashi Ishikawa[1a] and Shunichi Fukuzumi*[,1b]

Contribution from the Department of Applied Chemistry, Faculty of Engineering, Osaka University, Suita, Osaka 565, Japan. *Received May 25, 1990*

Abstract: 10-Methylacridine derivatives, 9,10-dihydro-10-methylacridine ($AcrH_2$) and acriflavine (AFH^+), act as efficient and stable photocatalysts in reductive dechlorination of *p*-chlorobiphenyl (ClBP) as well as dehalogenation of other halogenated compounds with sodium borohydride ($NaBH_4$) in a mixture of acetonitrile and H_2O (9:1 v/v) at 298 K. The reductive dechlorination proceeds via the reduction of ClBP by the singlet excited state ($^1AcrH_2^*$) to yield dechlorinated product (biphenyl) and 10-methylacridinium ion ($AcrH^+$), followed by the facile reduction of $AcrH^+$ with $NaBH_4$ to regenerate $AcrH_2$. The absence of the primary kinetic isotope effect as well as the comparison of the observed rate constants with those predicted by using the Marcus theory of electron transfer indicates that the reduction of halogenated compounds (RX) by the singlet excited state ($^1AcrH_2^*$) proceeds via photoinduced electron transfer from $^1AcrH_2^*$ to RX, which results in the cleavage of C-X bonds. In the photocatalytic reductive dehalogenation of *o*-, *m*-, and *p*-bromochlorobenzenes, cleavage of the C-Br bond predominates over that of the C-Cl bond in each case. In the case of halobenzyl halide ($X-C_6H_4CH_2X$; X = Cl, Br) only the CH_2-X bond is cleaved to yield halotoluene ($X-C_6H_4CH_3$) selectively.

Photochemical reductive dehalogenation of halogenated compounds, especially polychlorinated biphenyls (PCBs) has been studied extensively, in part due to their role as environmental pollutants.[2-8] Since direct irradiation of most halogenated compounds requires UV irradiation,[3-6] it is desired to use an appropriate photocatalyst which has sufficient spectral overlap with solar spectrum. Although several photocatalytic systems for reductive dehalogenation have been reported,[7,8] no photocatalyst has so far satisfied high efficiency and stability at the same time.

On the other hand, the carbon-halogen bond of halogenated compounds is known to be cleaved readily upon the one-electron reduction. Such dissociative electron transfer processes of halogenated compounds have been studied extensively by means of electrochemical techniques,[9-11] electron spin resonance (ESR),[12-14] and pulse radiolysis[15] for the detection of radical species formed upon the one-electron reduction of halogenated compounds. As such, the mechanisms of dissociative electron transfer have been well established,[9-15] and important parameters describing the energetics, such as the one-electron reduction potentials (E°_{red}) and the intrinsic barrier of electron transfer (the activation Gibbs energy at zero driving force) of both aliphatic and aromatic halides, are now available.[9-11] However, few applications of such dissociative electron transfer processes to appropriate photocatalytic systems have so far been reported. The mechanistic aspects of photocatalytic reductive dehalogenation also remain to be resolved.

This study reports efficient and stable photocatalytic systems for reductive dechlorination of *p*-chlorobiphenyl (ClBP), which is known to be one of the most difficult to be reduced among PCBs,[3f,5b] as well as dehalogenation of other halogenated compounds using sodium borohydride ($NaBH_4$) and 10-methylacridine derivatives [9,10-dihydro-10-methylacridine ($AcrH_2$) and acriflavine (AFH^+)] as a reductant and photocatalysts, respectively.

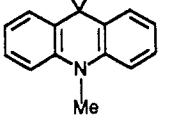

($AcrH_2$)

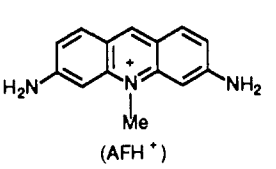

(AFH^+)

Mechanisms of the photocatalytic systems are discussed on the basis of the quantum yield determinations of both the photocatalytic reactions and the photoreduction of ClBP and other halogenated compounds by $AcrH_2$ (or AFH_2 which is the reduced

(1) (a) Current address: Laboratory of Organic Chemistry, Osaka Women's University, Sakai, Osaka 590, Japan. (b) To whom correspondence should be addressed at Osaka University.

(2) (a) Goldstein, J. A. *Top. Environ. Health* **1980**, *4*, 151. (b) Higuchi, K., Ed. *PCB Poisoning and Pollution*; Academic Press: Tokyo, 1976; pp 1-179. (c) Ackerman, D. G.; Scinto, L. L.; Bakshi, P. S.; Delumyea, R. G.; Johnson, R. J.; Richard, G.; Takata, A. M.; Sworzyn, E. M. *Destruction and Disposal of PCBs by Thermal and Non-Thermal Methods*; Noyes: Park Ridge, 1983.

(3) (a) Bunce, N. J.; Landers, J. P.; Langshaw, J. A.; Nakai, J. S. *Environ. Sci. Technol.* **1989**, *23*, 213. (b) Bunce, N. J.; Ravanal, L. *J. Am. Chem. Soc.* **1977**, *99*, 4150. (c) Bunce, N. J. *J. Org. Chem.* **1982**, *47*, 1948. (d) Bunce, N. J.; Kumar, Y.; Ravanal, L.; Safe, S. *J. Chem. Soc., Perkin Trans. 2* **1978**, 880. (e) Bunce, N. J.; Pilon, P.; Ruzo, L. O.; Sturch, D. J. *J. Org. Chem.* **1976**, *41*, 3023. (f) Bunce, N. J.; DeSchutter, C. T.; Toone, E. J. *J. Chem. Soc., Perkin Trans. 2* **1983**, 859.

(4) (a) Freeman, P. K.; Srinivasa, R.; Campbell, J.-A.; Deinzer, M. L. *J. Am. Chem. Soc.* **1986**, *108*, 5531, (b) Freeman, P. K.; Srinivasa, R. *J. Agric. Food Chem.* **1984**, *32*, 1313. (c) Freeman, P. K.; Ramnath, N. *J. Org. Chem.* **1988**, *53*, 148.

(5) (a) Epling, G. A.; Florio, E. *J. Chem. Soc., Chem. Commun.* **1986**, 185. (b) Epling, G. A.; Florio, E. *Tetrahedron Lett.* **1986**, *27*, 675. (c) Epling, G. A.; McVicar, W. M.; Kumar, A. *Chemosphere* **1988**, *17*, 1355.

(6) (a) Abeywickrema, A. N.; Beckwith, A. L. J. *Tetrahedron Lett.* **1986**, *27*, 109. (b) Beecroft, R. A.; Davidson, R. S.; Goodwin, D. *Tetrahedron Lett.* **1983**, *24*, 5673.

(7) (a) Ohashi, M.; Tsujimoto, K.; Seki, K. *J. Chem. Soc., Chem. Commun.* **1973**, 384. (b) Tsujimoto, K.; Tasaka, S.; Ohashi, M. *J. Chem. Soc., Chem. Commun.* **1975**, 758. (c) Ohashi, M.; Tsujimoto, K. *Chem. Lett.* **1983**, 423. (d) Tanaka, Y.; Tsujimoto, K.; Ohashi, M. *Bull. Chem. Soc. Jpn.* **1987**, *60*, 788. (e) Tanaka, Y.; Uryu, T.; Ohashi, M.; Tsujimoto, K. *J. Chem. Soc., Chem. Commun.* **1987**, 1703.

(8) (a) Soumillion, J. P.; Vandereecken, P.; De Schryver, F. C. *Tetrahedron Lett.* **1989**, *30*, 697. (b) Soumillion, J. P.; De Wolf, B. *J. Chem. Soc., Chem. Commun.* **1981**, 436.

(9) (a) Andrieux, C. P.; Blocman, C.; Dumas-Bouchiat, J. M.; Savéant, J.-M. *J. Am. Chem. Soc.* **1979**, *101*, 3431. (b) Andrieux, C. P.; Blocman, C.; Dumas-Bouchiat, J. M.; M'Halla, F.; Savéant, J.-M. *J. Am. Chem. Soc.* **1980**, *102*, 3806.

(10) (a) Andrieux, C. P.; Gallardo, I.; Savéant, J.-M.; Su, K.-B. *J. Am. Chem. Soc.* **1986**, *108*, 638. (b) Andrieux, C. P.; Savéant, J.-M.; Su, K. B. *J. Phys. Chem.* **1986**, *90*, 3815. (c) Savéant, J.-M. *J. Am. Chem. Soc.* **1987**, *109*, 6788.

(11) (a) Lund, T.; Lund, H. *Acta Chem. Scand.* **1986**, *B40*, 470. (b) Lund, T.; Lund, H. *Acta Chem. Scand.* **1987**, *B41*, 93. (c) Eberson, L.; Ekström, M.; Lund, T.; Lund, H. *Acta Chem. Scand.* **1989**, *43*, 101. (d) Lund, H.; Michel, M.-A.; Simonet, J. *Acta Chem. Scand.* **1974**, *B24*, 900.

(12) (a) Symons, M. C. R. *Pure Appl. Chem.* **1981**, *53*, 223. (b) Symons, M. C. R.; Bowman, W. R. *J. Chem. Soc., Perkin Trans. 2* **1988**, 583. (c) Mishra, S. P.; Symons, M. C. R. *J. Chem. Soc., Perkin Trans. 2* **1981**, 185.

(13) Russell, G. A.; Danen, W. C. *J. Am. Chem. Soc.* **1968**, *90*, 347.

(14) Namiki, A. *J. Chem. Phys.* **1975**, *62*, 990.

(15) (a) Neta, P.; Behar, D. *J. Am. Chem. Soc.* **1980**, *102*, 4798. (b) Neta, P.; Behar, D. *J. Am. Chem. Soc.* **1981**, *103*, 103. (c) Kigawa, H.; Takamuku, S.; Toki, S.; Kimura, N.; Takeda, S.; Tsumori, K.; Sakurai, H. *J. Am. Chem. Soc.* **1981**, *103*, 5176. (d) Norris, R. K.; Barker, S. D.; Neta, P. *J. Am. Chem. Soc.* **1984**, *106*, 3140. (e) Meot-Ner, M.; Neta, P.; Norris, R. K.; Wilson, K. *J. Phys. Chem.* **1986**, *90*, 168.

0002-7863/90/1512-8864$02.50/0

form of AFH^+), the fluorescence quenching by halogenated compounds, the primary kinetic isotope effects, and the comparison of the observed rate constants with those predicted by using the Marcus theory of electron transfer. We report also the selectivities of cleavage of carbon–halogen bonds of halogenated compounds containing different types of carbon–halogen bonds in the present photocatalytic system.

Experimental Section

Materials. 9,10-Dihydro-10-methylacridine ($AcrH_2$) was prepared from 10-methylacridinium iodide ($AcrH^+I^-$) by reduction with $NaBH_4$ in methanol and purified by recrystallization from ethanol.[16] The dideuteriated compound, [9,9′-$^2H_2$]-9,10-dihydro-10-methylacridine ($AcrD_2$), was prepared from 10-methylacridone by reduction with $LiAlD_4$,[17] which was obtained from Aldrich Chemical Co. Acriflavine (AFH^+), *p*-chlorobiphenyl (ClBP), *o*-, *m*-, and *p*-bromochlorobenzene, *o*-, *m*-, and *p*-chlorobenzyl chloride, *p*-bromobenzyl bromide, and other halogenated compounds were obtained commercially and purified by standard methods.[18] Sodium borohydride ($NaBH_4$) was obtained from Wako Pure Chemicals. Potassium ferrioxalate used as an actinometer was prepared according to the literature[19] and purified by recrystallization from hot water. Acetonitrile (MeCN) as well as acetonitrile-d_3 (CD_3CN) used as a solvent was purified by a standard procedure.[18]

Reaction Procedure. Typically, after a mixture of MeCN and H_2O (9:1 v/v, 0.5 mL) containing $AcrH_2$ (2.0×10^{-3} M), ClBP (1.0×10^{-1} M), and $NaBH_4$ (0.10–1.0 M)[20] in a square quartz cuvette (1 mm i.d.) was deaerated with a stream of argon, it was irradiated with the light from an Ushio Model UI-501 xenon lamp. All the resulting products were analyzed by GLC. The change of concentrations of $AcrH_2$ (λ_{max} = 285 nm) during the reaction was measured by using a Union SM-401 spectrophotometer.

The photoreduction of halogenated compounds by $AcrH_2$ was also carried out in the absence of $NaBH_4$. Typically, $AcrH_2$ (60 μmol) was added to an NMR tube that contained a CD_3CN solution (0.6 mL) of halogenated compounds (30 μmol). After the reactant solution in the NMR tube was deaerated, it was irradiated for about 10 h with light from a xenon lamp. The products were identified by comparison of their ^1H NMR spectra with those of authentic samples of $AcrH^+$ and dehalogenated compounds. The deuterium incorporation into products was also determined from the ^1H NMR spectra. The ^1H NMR measurements were carried out using a Japan Electron Optics JNM-PS-100 (100 MHz) or JNM-GSX-400 (400 MHz) NMR spectrometer.

Quantum-Yield Determinations. A standard actinometer (potassium ferrioxalate)[19] was used for the quantum yield determinations. The actinometry experiments were carried out under the same conditions as those of the photoreduction of halogenated compounds. Typically, after an MeCN/H_2O (9:1 v/v) solution (2.0 mL) containing $AcrH_2$ (2.0×10^{-3} M) and a halogenated compound in the absence or presence of $NaBH_4$ ($(1.0–2.0) \times 10^{-1}$ M)[20] in a square quartz cuvette (10 mm i.d.) was deaerated thoroughly with a stream of argon, it was irradiated with monochromatized light from a Ushio Model UXL-157 xenon lamp of a Hitachi 650-10S fluorescence spectrophotometer. The monochromatized wavelengths for the photochemical reactions of $AcrH_2$ and AFH_2 were selected normally as 320 nm and 350 nm, which are beyond the absorption due to halogenated compounds, respectively. The intensities of monochromatized light of λ = 320 nm (20-mm slit width) and λ = 350 nm (20-mm slit width) were determined as 2.2×10^{-6} and 2.4×10^{-6} einstein dm^{-3} s^{-1}, respectively. The quantum yields were determined from the rates of product formation (dehalogenated compounds and $AcrH^+$) by comparing with the incident light intensity absorbed by $AcrH_2$ and AFH_2. In most cases the concentrations of $AcrH_2$ were chosen such that approximately all the incident light was absorbed by $AcrH_2$. In the presence of $NaBH_4$, the absorption by $AcrH^+$ or AFH^+ was negligible, since the facile reduction of $AcrH^+$ or AFH^+ by $NaBH_4$ occurred during the photocatalytic reactions. In the case of photoreduction of halogenated compounds by $AcrH_2$ in the absence of $NaBH_4$, the quantum yields were determined from the initial rate of formation of $AcrH^+$ under the conditions that the light absorption by $AcrH^+$ can be neglected as compared to that by $AcrH_2$. The light absorption of chlorinated compounds was negligible at the irradiation wavelength of λ > 320 nm. At high concentrations of halogenated compounds such as alkyl iodides, however, the absorption by the halogenated compounds were taken into account in determining the quantum yields of the photoreduction by $AcrH_2$. The concentrations of products were determined by GLC as well as the electronic spectra.

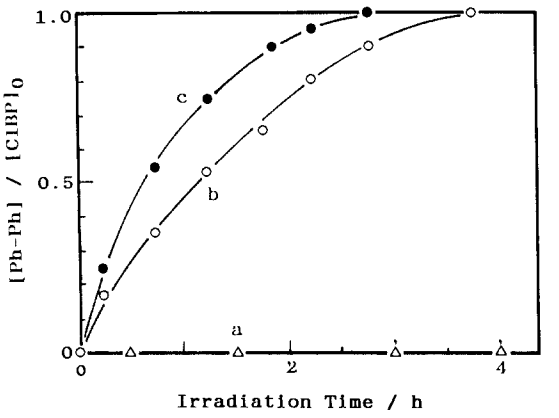

Figure 1. Photodechlorination of ClBP (0.10 M) with $NaBH_4$ (1.0 M) (a) in the absence of catalyst (△), (b) in the presence of $AcrH_2$ (2.0×10^{-2} M) (○), and (c) AFH^+ (2.0×10^{-2} M) (●) in a mixture of MeCN and H_2O (9:1 v/v) at 298 K under irradiation of light from a xenon lamp. Plots of ratio of the product concentration [Ph–Ph] to the initial ClBP concentration $[ClBP]_0$ vs irradiation time.

Fluorescence Quenching. Fluorescence measurements were carried out on a Hitachi 650-10S fluorescence spectrophotometer. In the fluorescence quenching experiments, the excitation wavelengths beyond the quencher absorption were selected normally as 320 nm and 350 nm for $AcrH_2$ and AFH_2, respectively. Relative fluorescence intensities were measured for deaerated MeCN/H_2O (9:1 v/v) solutions of $AcrH_2$ (or AFH^+) with a quencher at various concentrations in the presence of $NaBH_4$ (1.0×10^{-1} M).[20] Relative fluorescence intensities were measured also for deaerated MeCN solutions of $AcrH_2$ (1.0×10^{-5} M) with a quencher at various concentrations in the absence of $NaBH_4$. There was no change in the shape but there was a change in the intensity of the fluorescence spectrum by the addition of a quencher. The Stern–Volmer relationship (eq 1) was obtained for the ratio of the fluorescence intensities in the absence and presence of a quencher (I_0/I) and the concentrations of halogenated compounds used as quenchers [RX]. The fluorescence lifetime τ of $AcrH_2$ was determined as 7.0 ns in MeCN by single photon counting by using a Horiba fluorescence lifetime apparatus (NAES-1100). The τ value in the presence of H_2O [MeCN/H_2O (9:1 v/v)] was the same as that in its absence. The observed quenching rate constants k_q ($=K_{SV}\tau^{-1}$) was obtained from the Stern–Volmer constant K_{SV} and the fluorescence lifetime τ.

$$I_0/I = 1 + K_{SV}[RX] \quad (1)$$

Results and Discussion

Photoreduction of ClBP by $NaBH_4$ Catalyzed by Acridine Derivatives. No appreciable photoreduction of ClBP by $NaBH_4$ occurs in the absence of photocatalyst in a mixture of acetonitrile and H_2O (MeCN/H_2O, 9:1 v/v) under irradiation of light from a xenon lamp as shown in Figure 1 (part a).[21] When 9,10-dihydro-10-methylacridine ($AcrH_2$) or acriflavine (AFH^+) is added to this system at 298 K, each species acts as an efficient photocatalyst for reductive dechlorination of ClBP with $NaBH_4$ to yield biphenyl as shown in Figure 1 (parts b and c, respectively). The formation of biphenyl was identified by GLC (see Experimental Section). When $AcrH_2$ was replaced by the oxidized form, 10-methylacridinium perchlorate ($AcrH^+ClO_4^-$), essentially the same result was obtained, since $AcrH^+$ was immediately reduced by $NaBH_4$ to yield $AcrH_2$ selectively.[16] Similarly AFH^+ was readily converted to the reduced form (AFH_2) by the reduction by

(16) Roberts, R. M. G.; Ostovič, D.; Kreevoy, M. M. *Faraday Discuss. Chem. Soc.* **1982**, *74*, 257.

(17) (a) Ostovič, D.; Roberts, R. M. G.; Kreevoy, M. M. *J. Am. Chem. Soc.* **1983**, *105*, 7629. (b) Karrer, P.; Szabo, L.; Krishna, H. J. V.; Schwyzer, R. *Helv. Chim. Acta* **1950**, *33*, 294.

(18) Perrin, D. D.; Armarego, W. L. F.; Perrin, D. R. *Purification of Laboratory Chemicals*; Pergamon Press: New York, 1966.

(19) (a) Hatchard, C. G.; Parker, C. A. *Proc. R. Soc. London, Ser. A* **1956**, *235*, 518. (b) Calvert, J. G.; Pitts, J. N. *Photochemistry*; Wiley: New York, 1966; p 783.

(20) In the presence of high concentrations of $NaBH_4$ (e.g., 1.0 M), a mixture of MeCN and H_2O (9:1 v/v) separates into two phases. Thus, the quantum yield as well as the fluorescence measurments in the presence of $NaBH_4$ were performed at the lower concentrations.

(21) The photolysis with a Ushio model UI-501 xenon lamp results in no appreciable reaction under our experimental conditions although photolysis of ClBP and $NaBH_4$ with a low-pressure mercury lamp is reported to result in the dechlorination of ClBP.[5b]

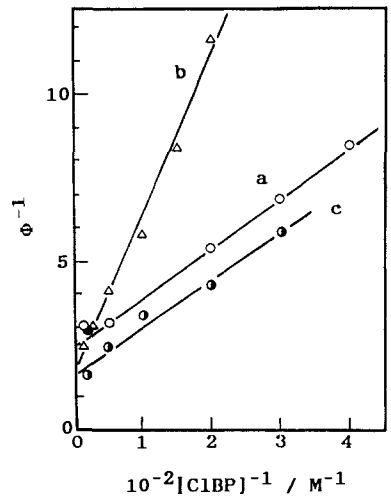

Figure 2. Plots of Φ^{-1} vs $[ClBP]^{-1}$ for photodechlorination of ClBP (a) in the presence of $AcrH_2$ (2.0×10^{-3} M) and $NaBH_4$ (2.0×10^{-1} M) (○), in the presence of $AcrH^+$ (2.0×10^{-3} M) and $NaBH_4$ (1.0×10^{-1} M) (●) under irradiation of light of λ 320 nm, (b) in the presence of AFH^+ (2.0×10^{-2} M) and $NaBH_4$ (1.0×10^{-1} M) under irradiation of light λ 350 nm (△), and (c) in the presence of $AcrH_2$ (2.0×10^{-3} M) without $NaBH_4$ under irradiation of light λ 320 nm (◑) in $MeCN/H_2O$ (9:1 v/v) at 298 K.

$NaBH_4$. No appreciable photodegradation of the catalysts has been observed during the photocatalytic reaction, since the concentration of $AcrH_2$ or AFH_2 remains unchanged during the photocatalytic reactions. Thus, both $AcrH_2/AcrH^+$ and AFH_2/AFH^+ redox pairs act as not only efficient but also stable photocatalysts for dechlorination of ClBP with $NaBH_4$.

The quantum yields (Φ) of the photocatalytic dechlorination of ClBP were determined by using a ferrioxalate actinometer (see Experimental Section). The Φ values in the presence of $AcrH_2$ under irradiation of light of λ = 320 nm were constant with the change of both $AcrH_2$ and $NaBH_4$ concentrations. On the other hand, the quantum yield increased with an increase in the concentration of ClBP to approach a limiting value (Φ_∞) in the high concentrations in accordance with eq 2, where K_{obs} is the observed quenching constant of the excited state involved in the photocatalytic reaction. Equation 2 can be rewritten as eq 3, which

$$\Phi = \Phi_\infty K_{obs}[ClBP]/(1 + K_{obs}[ClBP]) \quad (2)$$

$$\Phi^{-1} = \Phi_\infty^{-1}[1 + (K_{obs}[ClBP])^{-1}] \quad (3)$$

predicts a linear correlation between Φ^{-1} and [ClBP]. Such a linear correlation is confirmed for the photocatalytic reduction of ClBP by $NaBH_4$ in the presence of $AcrH_2$ as shown in Figure 2 (part a). From the linear plot are obtained the Φ_∞ and K_{obs} values as listed in Table I. When $AcrH_2$ is replaced by $AcrH^+ClO_4^-$, essentially the same Φ value is obtained as shown in Figure 2 (part a), since $AcrH^+$ is readily converted to $AcrH_2$ by the reduction with $NaBH_4$ (vide supra). A linear correlation between Φ^{-1} and $[ClBP]^{-1}$ is also obtained for the photocatalytic reduction of ClBP by $NaBH_4$ in the presence of AFH^+ under irradiation of light of λ = 350 nm as shown in Figure 2 (part b). The Φ_∞ value determined for the AFH_2/AFH^+ catalytic system (Φ_∞ = 0.63) from the plot in Figure 2 (part b) is larger than the Φ_∞ value of the $AcrH_2/AcrH^+$ system (0.42), but the K_{obs} value (3.3×10^1 M^{-1}) is smaller than that of the latter system (1.6×10^2 M^{-1}) as shown in Table I.

In the absence of $NaBH_4$, the stoichiometric reduction of ClBP by $AcrH_2$ in $MeCN/H_2O$ (9:1 v/v) under irradiation of light of λ = 320 nm occurs to yield biphenyl and $AcrH^+$ (eq 4). The

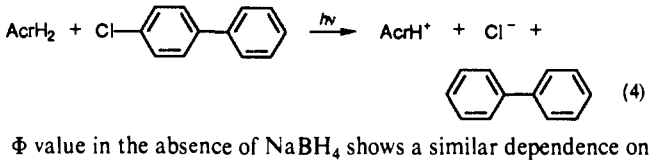

(4)

Φ value in the absence of $NaBH_4$ shows a similar dependence on [ClBP] to the Φ value in the presence of $NaBH_4$. Thus, a linear correlation between Φ^{-1} and $[ClBP]^{-1}$ (eq 3) is also obtained for the stoichiometric photoreduction of ClBP by $AcrH_2$ as shown in Figure 2 (part c). The Φ_∞ and K_{obs} values, determined from the plot in Figure 2 (part c), agree reasonably well with those obtained for the catalytic reaction in the presence of $NaBH_4$ (Table I).[22]

Table I. Limiting Quantum Yields (Φ_∞) and the Observed Quenching Constants K_{obs} of the Excited States Involved in the Photoreduction of ClBP in the Presence of $AcrH_2$ (2.0×10^{-3} M) or AFH^+ (2.0×10^{-2} M) in $MeCN/H_2O$ (9:1 v/v) at 298 K, and the Stern–Volmer Constants (K_{SV}) for the Fluorescence Quenching of $^1AcrH_2^*$ and $^1AFH_2^*$ by ClBP in $MeCN/H_2O$ (9:1 v/v) at 298 K

acridine derivative	in the presence of $NaBH_4$		in the absence of $NaBH_4$		in the presence of $NaBH_4$
	Φ_∞[a,b]	K_{obs}[a,b] M^{-1}	Φ_∞[a,b]	K_{obs}[a,b] M^{-1}	K_{SV}[b,c] M^{-1}
$AcrH_2$[d]	0.42	1.6×10^2	0.61	1.2×10^2	1.2×10^2
AFH^+[e]	0.63	3.3×10^1	-	-	3.6×10^1

[a] Determined from the plots in Figure 2. [b] Determined from the Stern–Volmer plots for the fluorescence quenching. [c] The experimental errors are within ±10%. [d] The irradiation wavelength is 320 nm; [$NaBH_4$] = 2.0×10^{-1} M. [e] The irradiation wavelength is 350 nm; [$NaBH_4$] = 1.0×10^{-1} M.

Scheme I

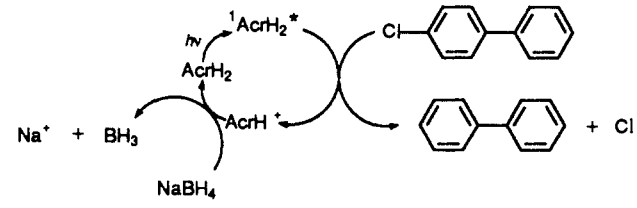

Since the one-electron oxidation potential (E°_{ox}) of the singlet excited state $^1AcrH_2^*$ is known to be largely negative (E°_{ox} = −3.1 V vs SCE),[23] $^1AcrH_2^*$ may act as a very strong reductant. In fact, the fluorescence of $^1AcrH_2^*$ as well as $^1AFH_2^*$ is readily quenched by ClBP. The fluorescence quenching may be a dynamic process, since no complex formation is observed between ClBP and $AcrH_2$ as well as AFH_2. From the Stern–Volmer plots are obtained the Stern–Volmer constants (K_{SV}) of $^1AcrH_2^*$ and $^1AFH_2^*$ as listed in Table I (1.2×10^2 M^{-1} and 3.6×10^1 M^{-1}, respectively). The K_{SV} values of $^1AcrH_2^*$ and $^1AFH_2^*$ agree well with the K_{obs} values determined from the plots of Φ^{-1} vs $[ClBP]^{-1}$ (eq 3) for the photoreduction of ClBP with $AcrH_2$ and AFH_2 in the presence and absence of $NaBH_4$ (Table I). Such agreements of K_{SV} and K_{obs} values indicate that the photocatalytic dechlorination of ClBP by $NaBH_4$ proceeds via the reductive dechlorination of ClBP by the singlet excited states $^1AcrH_2^*$ (or $^1AFH_2^*$), followed by the facile thermal reduction of $AcrH^+$ (or AFH^+) with $NaBH_4$ to regenerate $AcrH_2$ (or AFH_2) as shown in Scheme I.

Photoreduction of Halogenated Compounds by $AcrH_2$ via Photoinduced Electron Transfer. In the absence of $NaBH_4$, the stoichiometric reduction of various halogenated compound (RX; X = I, Br, and Cl) by $AcrH_2$ occurs also in MeCN under irradiation of light of λ = 320 nm to yield RH and $AcrH^+$. When $AcrH_2$ is replaced by the 9,9′-dideuteriated analogue ($AcrD_2$), the deuterium is incorporated into the dehalogenated product (see Experimental Section, eq 5).[24] As the case of ClBP (eq 3), the

$$AcrD_2 + RX \xrightarrow{h\nu} AcrD^+ + RD + X^- \quad (5)$$

$$\Phi^{-1} = \Phi_\infty^{-1}[1 + (K_{obs}[RX])^{-1}] \quad (6)$$

(22) The limiting quantum yields in the presence of $NaBH_4$ may be larger than the observed value 0.42, since the photolysis in the presence of $NaBH_4$ results in the formation of H_2 which bubbles up from the reactant solution, causing the slight decrease in the light absorption, which is not taken account in determining the Φ values.

(23) Fukuzumi, S.; Tanaka, T. *Photoinduced Electron Transfer*; Fox, M. A., Chanon, M., Ed.; Elsevier: Amsterdam, 1988; Part C, Chapter 10.

Table II. Observed Rate Constants (k_q) for the Reactions of $^1AcrH_2$* and $^1AcrD_2$* with RX in MeCN at 298 K, Calculated Rate Constants of Electron Transfer from $^1AcrH_2$* to RX, and the Gibbs Energy Change ($\Delta G°_{et}$) and Intrinsic Barrier ($\Delta G^‡_0$) of the Electron Transfer

RX	$\Delta G°_{et}$,[a] kcal mol^{-1}	$\Delta G^‡_0$,[b] kcal mol^{-1}	$k_q(AcrH_2)$,[c] M^{-1} s^{-1}	$k_q(AcrD_2)$,[c] M^{-1} s^{-1}	k_{et},[d] M^{-1} s^{-1}
PhCl	−7.4[e]	5.8[e]	6.0×10^8	6.2×10^8	5×10^8
p-CNC_6H_4Cl	−21.2[e]	5.8[g]	2.2×10^{10}	2.2×10^{10}	2×10^{10}
PhBr	−15.2[e]	6.3[e]	1.2×10^9	–	7×10^9
PhI	–	–	2.6×10^{10}	2.7×10^{10}	–
$PhCH_2Cl$	−50.9[f]	18.3[h]	3.0×10^9	2.7×10^9	4×10^9
CCl_4	−52.5[f]	11.7[i]	3.2×10^{10}	–	2×10^{10}
$CHCl_3$	–	–	2.0×10^{10}	–	–
CH_2Cl_2	–	–	3.8×10^8	3.3×10^8	–
C_3H_7Br	−44.5[f]	17.7[j]	4.6×10^8	4.6×10^8	1×10^9
C_2H_5Br	−45.2[f]	17.7[j]	7.0×10^8	6.4×10^8	1×10^9
$PhCH_2Br$	−55.3[f]	17.7[j]	2.6×10^{10}	–	1×10^{10}
C_4H_9I	−43.6[f]	14.5[k]	1.7×10^{10}	–	9×10^9
CH_3I	−41.2[f]	14.5[l]	1.8×10^{10}	–	7×10^9
C_2H_5I	−44.7[f]	14.5[l]	1.8×10^{10}	–	1×10^{10}

[a] Obtained from the $E°_{ox}$ and $E°_{red}$ values of $^1AcrH_2$* (refs 23 and 26) and RX by using eq 8, respectively. [b] Assumed to be the same as those reported for electron transfer from aromatic radical anions to RX. [c] The experimental errors are ±10%. [d] Calculated by using eqs 7–9 (see text). [e] The $E°_{red}$ values are taken from ref 9. [f] The $E°_{red}$ values are taken from ref 27. [g] Assumed to the same as that of PhCl. [h] Taken from ref 11b. [i] Obtained from the data reported in ref 11c by using eq 7. [j] Assumed to be the same as that of C_4H_9Br (ref 10), since the simple alkyl halides are known to have similar $\Delta G^‡_0$ values (ref 11a). [k] Taken from ref 10. [l] Assumed to be the same as that of C_4H_9I.

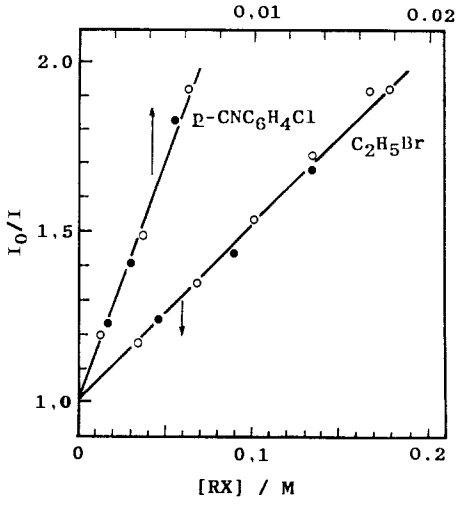

Figure 3. Stern–Volmer plots for fluorescence quenching of $^1AcrH_2$*(○) and $^1AcrD_2$*(●) with *p*-CNC_6H_4Cl and C_2H_5Br in MeCN at 298 K.

linear corrclation between Φ^{-1} and $[RX]^{-1}$ are also obtained (eq 6). The fluorescence of $AcrH_2$ is also quenched efficiently with RX. From the Stern–Volmer plots are obtained the Stern–Volmer constants (K_{SV}) which agree well with the K_{obs} values obtained from the plots of Φ^{-1} and $[RX]^{-1}$ as observed in the case of ClBP (Table I). Thus, the observed quenching rate constants (k_q) are obtained from the fluorescence lifetime τ and K_{SV} (or K_{obs}) by using the relation, $k_q = K_{SV}\tau^{-1}$ (or $K_{obs}\tau^{-1}$). Typical Stern–Volmer plots for both $AcrH_2$ and the 9,9′-dideuteriated analogue ($AcrD_2$) are shown in Figure 3, where no appreciable primary kinetic isotope effects are observed. The k_q and Φ_∞ values of both $AcrH_2$ and $AcrD_2$, thus obtained are summarized in Table II and Table III, respectively.

The absence of primary kinetic isotope effects on both k_q and Φ_∞ (Tables II and III) suggests that the quenching of $^1AcrH_2$* with RX may be electron transfer from $^1AcrH_2$* to RX. The activation Gibbs energy ($\Delta G^‡_{et}$) of such electron transfer may be calculated by using the Marcus equation (eq 7),[25] where $\Delta G°_{et}$

$$\Delta G^‡_{et} = \Delta G^‡_0[1 + (\Delta G°_{et}/4\Delta G^‡_0)]^2 \quad (7)$$

is the standard Gibbs energy change of electron transfer and $\Delta G^‡_0$ is $\Delta G^‡_{et}$ at zero driving force ($\Delta G°_{et} = 0$). The $\Delta G°_{et}$ values of

Table III. Limiting Quantum Yields (Φ_∞) of the Photoreduction of Halogenated Compounds (RX) by $AcrH_2$ and $AcrD_2$ in MeCN at 298 K and the Gibbs Energy Change ($\Delta G°_{be}$) of Back Electron Transfer from $RX^{\bullet-}$ to $AcrH_2$

RX	$\Delta G°_{be}$,[a] kcal mol^{-1}	$\Phi_\infty(AcrH_2)$[b]	$\Phi_\infty(AcrD_2)$[b]
PhCl	−83	0.12	0.12
p-CNC_6H_4Cl	−69	0.17	0.17
PhBr	−76	0.20	–
PhI	–	0.21	0.20
$PhCH_2Cl$	−39	0.21	0.21
CCl_4	−37	0.34	–
$CHCl_3$	–	0.27	0.27
CH_2Cl_2	–	0.17	0.17
C_3H_7Br	−45	0.20	–
C_2H_5Br	−45	0.15	0.13
C_4H_9I	−46	0.32	–
$PhCH_2Br$	−35	0.31	–
CH_3I	−49	0.12	–
C_2H_5I	−45	0.15	–

[a] Obtained from the $E°_{ox}$ and $E°_{red}$ values of $AcrH_2$ (ref 26) and RX (refs 9 and 27) by using eq 8. [b] The experimental errors are ±10%.

electron transfer from $^1AcrH_2$* to RX are obtained from the oxidation potential of the singlet excited state $^1AcrH_2$* ($E°_{ox}$ = −3.1 V vs SCE)[23,26] and the one-electron reduction potentials of RX ($E°_{red}$)[9-11,27] by using eq 8, where F is the Faraday constant.

$$\Delta G°_{et} = F(E°_{ox} - E°_{red}) \quad (8)$$

With regard to the intrinsic barrier for the one-electron reduction of RX, the $\Delta G^‡_0$ values of electron transfer from electrogenerated aromatic radical anions to various halogenated compounds have been reported.[9-11] The reported $\Delta G^‡_0$ values may be applied directly to the present case, since the intrinsic barrier for the one-electron oxidation of various aromatic radical anions being constant are similar to that of $AcrH_2$.[23,26] The $\Delta G°_{et}$ and $\Delta G^‡_0$ values thus obtained are listed in Table II.[28] On the other hand, the rate constant of photoinduced electron transfer (k_{et}) is known to be given as a function of $\Delta G^‡_{et}$ and $\Delta G°_{et}$ (eq 9).[29] The k_{et}

$$k_{et} = (2.0 \times 10^{10})/[1 + 0.25[\exp(\Delta G^‡_{et}/RT) + \exp(\Delta G°_{et}/RT)]] \quad (9)$$

(24) In the case of $CHCl_3$, the dechlorinated product was obtained as $CDHCl_2$ (see Experimental Section).

(25) (a) Marcus, R. A. *J. Chem. Phys.* **1965**, *43*, 679. (b) Marcus, R. A. *Ann. Rev. Phys. Chem.* **1964**, *15*, 155.

(26) Fukuzumi, S.; Koumitsu, S.; Hironaka, K.; Tanaka, T. *J. Am. Chem. Soc.* **1987**, *109*, 305.

(27) Eberson, L. *Acta Chem. Scand.* **1982**, *B36*, 533.

(28) The $E°_{red}$ values in DMF[9,10,27] are used to obtain the $G°_{et}$ values, since the most reported $\Delta G^‡_0$ values have been determined in DMF.[9-11] The use of the $E°_{red}$ and $\Delta G°_{et}$ values in DMF instead of those in MeCN may be justified, since no significant difference in the rate constants of electron transfer from aromatic radical anions to RX in MeCN and DMF has been observed.[11a]

Scheme II

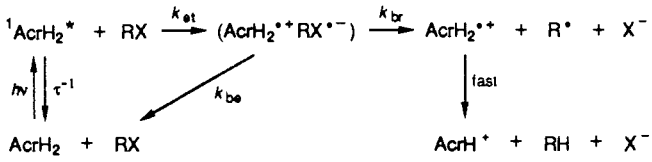

values calculated from the $\Delta G°_{et}$ and $\Delta G_0^{\ddagger}$ values in Table II by using eqs 7 and 9 are also listed in Table II.

If uncertainties in the $\Delta G°_{et}$ and $\Delta G_0^{\ddagger}$ values are taken into account, reasonable agreement between k_{et} and k_q combined with the absence of the primary kinetic isotope effects on k_q (Table II) strongly indicates that the photoreduction of RX by $AcrH_2$ proceeds via photoinduced electron transfer from $^1AcrH_2^*$ to RX as shown in Scheme II. It is well known that the one-electron reduction of RX results in the cleavage of C–X bond to give R$^\bullet$ and X^-.[9-15] Thus, the photoinduced electron transfer from $^1AcrH_2^*$ to RX may be followed by the fast hydrogen transfer from $AcrH_2^{\bullet+}$ to R$^\bullet$, yielding $AcrH^+$ and RH (Scheme II).[30] In the case of aromatic halides the radical anions ($RX^{\bullet-}$) are generally believed to have a finite lifetime.[10,12,14] In such a case the bond-breaking process of $RX^{\bullet-}$ (k_{br}) yielding the dehalogenated products may compete with the back-electron-transfer process (k_{be}) from $ArX^{\bullet-}$ to $AcrH_2^{\bullet+}$ (Scheme II). By applying the steady-state approximation to the reactive intermediates, $^1AcrH_2^*$ and ($AcrH_2^{\bullet+}$ $RX^{\bullet-}$) in Scheme II, the dependence of Φ on [RX] can be derived as given by eq 10, which agrees with the experimental results in eq 6 (or eq 2). By comparing eqs 6 and 10 the limiting quantum yield (Φ_∞) may be given by eq 11. The absence of

$$\Phi = k_{et}\tau k_{br}[RX]/(1 + k_{et}\tau[RX])(k_{br} + k_{be}) \quad (10)$$

$$\Phi_\infty = k_{br}/(k_{br} + k_{be}) \quad (11)$$

primary kinetic isotope effects on Φ_∞ values in Table III also supports eq 11, where no hydrogen transfer process is involved. According to eq 11, the Φ_∞ value may be determined by the competition between the bond-breaking process (k_{br}) and the back-electron-transfer process (k_{be}). The Gibbs energy change of the back electron transfer from $RX^{\bullet-}$ to $AcrH_2^{\bullet+}$ ($\Delta G°_{be}$) is obtained from the one-electron oxidation potential of $AcrH_2^{\bullet+}$ ($E°_{ox}$ = 0.80 V vs SCE)[26,31] and the one-electron reduction potentials of RX ($E°_{red}$).[9,27] The $\Delta G°_{be}$ values thus obtained are also listed in Table III.

It has been reported that the lifetime of radical anions of aromatic halides (k_{br}^{-1}) increases generally with the positive shift of the one-electron-reduction potentials of aromatic halides.[10b] Unlike the case of aromatic halides, radical anions of alkyl halides are generally believed to have no detectable lifetime.[10,32-34] In this case as well, the lifetime may increase with the positive shift of the one-electron-reduction potentials of alkyl halides, since the discreet radical anions of alkyl halides with electron withdrawing

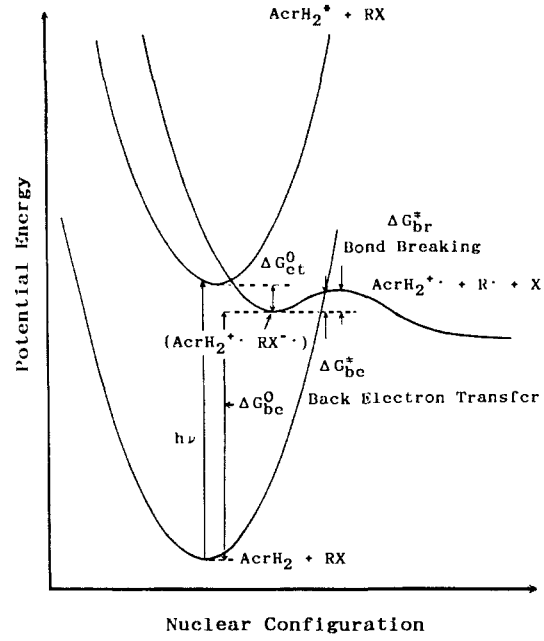

Figure 4. Qualitative potential energy curves for photoinduced electron transfer from $^1AcrH_2^*$ to RX emphasizing the similarity of the energetic barrier of back electron transfer from $RX^{\bullet-}$ to $AcrH_2^{\bullet+}$ and that of C–X bond breaking of $RX^{\bullet-}$.

Scheme III

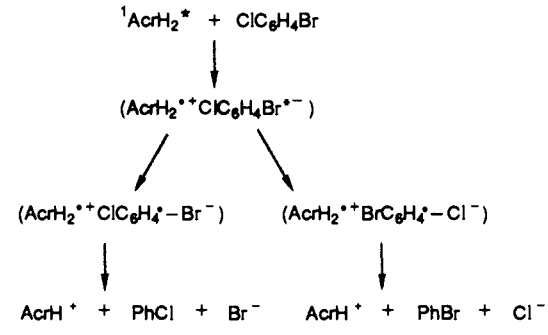

substituents such as $CCl_4^{\bullet-}$ and $CF_3X^{\bullet-}$ are known to exist.[35,36] Thus, the k_{br} values of radical anions of halogenated compounds in Table III, where the Gibbs energy change of back electron transfer from $RX^{\bullet-}$ to $AcrH_2^{\bullet+}$ ($\Delta G°_{be}$) spanning a wide range are expected to vary significantly. In this context, the rather constant Φ_∞ values in Table III (0.12–0.32) may at first sight seem surprising. However, the k_{be} value may also vary in parallel with the k_{br} value. This possibility is indicated in Figure 4, which displays the plausible energy surface profiles of photoinduced electron transfer from $^1AcrH_2^*$ to RX schematically.[37] Initially, excitation of $AcrH_2$ brings the reactant system to an excited-state energy surface where thermal equilibration into a lower vibration state is rapidly established. Following electron transfer, nuclear relaxation rapidly established the thermally equilibrated radical ion pair ($AcrH_2^{\bullet+}$ $RX^{\bullet-}$). The stretching of R–X bond of $RX^{\bullet-}$ by surmounting the bond breaking barrier ($\Delta G_{br}^{\ddagger}$) yields the products ($AcrH_2^{\bullet+}$, R$^\bullet$, and X^-). When the back electron transfer from $RX^{\bullet-}$ to $AcrH_2^{\bullet+}$ is highly exergonic ($\Delta G°_{be} \ll 0$) as shown in Table III, the activation Gibbs energy of back electron transfer ($\Delta G_{be}^{\ddagger}$) may be close to that of bond-breaking process ($\Delta G_{br}^{\ddagger}$) as shown in Figure 4.[38-40] Thus, irrespective of the magnitude of

(29) (a) Rehm, D.; Weller, A. *Isr. J. Chem.* **1970**, *8*, 259. (b) Rehm, D.; Weller, A. *Ber. Bunsenges. Phys. Chem.* **1969**, *73*, 834. (c) Indelli, M. T.; Scandola, F. *J. Am. Chem. Soc.* **1978**, *100*, 7733.

(30) Alternatively, proton transfer from $AcrH_2^{\bullet+}$ to $RX^{\bullet-}$ may occur, followed by the subsequent electron transfer from AcrH$^\bullet$ to yield the dehalogenated products as reported for the photoreduction of phenacyl halides by $AcrH_2$; see: Fukuzumi, S.; Mochizuki, S.; Tanaka, T. *J. Chem. Soc., Perkin Trans. 2* **1989**, 1583.

(31) A similar $E°_{ox}$ value ($E°_{ox}$ = 0.86 V) has recently been reported; see: Hapiot, P.; Moiroux, J.; Savéant, J.-M. *J. Am. Chem. Soc.* **1990**, *112*, 1337.

(32) (a) Mishra, S. P.; Symons, M. C. R. *J. Chem. Soc., Perkin Trans. 2* **1973**, 391. (b) Sprague, E. D.; Williams, F. *J. Chem. Phys.* **1971**, *54*, 5425. (c) Symons, M. C. R.; Smith, I. G. *J. Chem. Soc., Perkin Trans. 2* **1981**, 1180. (d) Symons, M. C. R. *J. Chem. Soc., Perkin Trans. 2* **1972**, 1397. (e) Fujita, Y.; Katsu, T.; Sato, M.; Takahashi, K. *J. Chem. Phys.* **1974**, *61*, 4307.

(33) (a) Irie, M.; Shimizu, M.; Yoshida, H. *J. Phys. Chem.* **1976**, *80*, 2008. (b) Izumida, T.; Ichikawa, T.; Yoshida, H. *J. Phys. Chem.* **1980**, *84*, 60. (c) Izumida, T.; Fujii, K.; Ogasawara, M.; Yoshida, H. *Bull. Chem. Soc. Jpn.* **1983**, *56*, 82.

(34) For the discussion whether the radical anions of alkyl halides have a finite lifetime or not; see: Symons, M. C. R. *J. Chem. Res. (S)* **1978**, 360. Garst, J. F.; Roberts, R. D.; Pacifici, J. A. *J. Am. Chem. Soc.* **1977**, *99*, 3528.

(35) (a) Klassen, N. V.; Ross, C. K. *J. Phys. Chem.* **1987**, *91*, 3668. (b) Klassen, N. V.; Ross, C. K. *Chem. Phys. Lett.* **1986**, *132*, 478.

(36) (a) Shiotani, M.; Williams, F. *J. Am. Chem. Soc.* **1976**, *98*, 4006. (b) Wang, J. T.; Williams, F. *J. Am. Chem. Soc.* **1980**, *102*, 2860.

(37) Electron transfer from $^1AcrH_2^*$ to RX may be adiabatic, although no splitting at the crossing point between the reaction and product potential surfaces is shown in the simplified figure.

Scheme IV

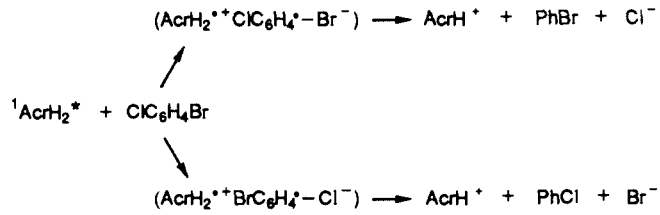

Table IV. Selectivity (%) of Photocatalytic Reductive Dehalogenation of Halogenated Compounds (2.0×10^{-1} M) by $NaBH_4$ (2.0×10^{-1} M) in the Presence of $AcrH_2$ (2.0×10^{-3} M) under Irradiation of Light $\lambda = 320$ nm in $MeCN/H_2O$ (9:1 v/v) at 298 K

halogenated compound	product,[a] %
o-BrC_6H_4Cl	PhCl (89), PhBr (11)
m-BrC_6H_4Cl	PhCl (94), PhBr (6)
p-BrC_6H_4Cl	PhCl (87), PhBr (13)
o-$ClC_6H_4CH_2Cl$	*o*-$ClC_6H_4CH_3$ (100)
m-$ClC_6H_4CH_2Cl$	*m*-$ClC_6H_4CH_3$ (100)
p-$ClC_6H_4CH_2Cl$	*p*-$ClC_6H_4CH_3$ (100)
p-$BrC_6H_4CH_2Br$	*p*-$BrC_6H_4CH_3$ (100)

[a] Determined by GLC at low conversions (<10%).[43]

$\Delta G^{\ddagger}_{br}$ (or lifetime of $RX^{\bullet-}$) the approximate relation $\Delta G^{\ddagger}_{br} \simeq \Delta G^{\ddagger}_{be}$ ($k_{br} \simeq k_{be}$) may always hold, when the Φ_∞ value $[k_{br}/(k_{br} + k_{be})]$ is approximately constant being close to 0.5 as observed in Tables I and III (0.12–0.63).[41]

Selectivities of Reductive Dehalogenation. With regard to radical anions of aromatic halides both the π^* and σ^* radicals which differ in the orbital occupied by the unpaired electron (π^* and σ^* denote that the unpaired electron lies in the π^* and σ^* type orbitals, respectively) are known to exist.[12] If electron is transferred initially to the π^* orbital of ArX, the σ bond breaking may occur via intramolecular electron transfer from the π^* to σ^* orbital, the energy barrier of which may correspond to that of the bond-breaking process.[10b] Alternatively, an electron may be transferred directly to the σ^* orbitals to yield the σ^* radicals.[42] The distinction whether the π^* radicals are intermediates for the formation of σ^* radicals or not may be achieved by examining the selectivities in the reductive dehalogenation of aromatic halides containing different C–X bonds (vide infra). In the former case photoinduced electron transfer from $^1AcrH_2^*$ to ClC_6H_4Br gives the corresponding π^* radical anions which are converted to different σ^* radical anions, $ClC_6H_4^{\bullet}$–Br^- and $BrC_6H_4^{\bullet}$–Cl^- to yield chlorobenzene and bromobenzene, respectively (Scheme III). In this case the selectivities of the reductive dehalogenation may be determined by the competition of intramolecular electron transfer from the π^* to σ^* orbitals of the C–Cl and C–Br bonds. In the latter case the selectivities may be determined by the competition of initial electron transfer from $^1AcrH_2^*$ to the C–Br and C–Cl σ^* orbitals of ClC_6H_4Br (Scheme IV).

The selectivities of reductive dehalogenation of bromochlorobenzenes (*o*-, *m*-, and *p*-ClC_6H_4Br) were determined by the product ratio of PhBr and PhCl in the $AcrH_2/AcrH^+$-catalyzed photoreduction of ClC_6H_4Br with $NaBH_4$ in $MeCN/H_2O$ (9:1 v/v) under irradiation of light of $\lambda = 320$ nm.[43] The concentrations of ClC_6H_4Br (0.20 M) were chosen such that the quantum yields are close to the limiting values (Φ_∞). The results of the selectivities of reductive dehalogenation of *o*-, *m*-, and *p*-ClC_6H_4Br are summarized in Table IV, where PhCl is obtained as a major product in each case.[44] If the reductive dehalogenation of Cl-C_6H_4Br proceeds by direct formation of the σ^* radical anions (Scheme IV), the rates of reductive debromination of ClC_6H_4Br would be comparable to those of reductive dechlorination, judging from the similar Φ_∞ values of reductive debromination of PhBr and dechlorination of PhCl (Table III). Thus, selective debromination of ClC_6H_4Br as compared to the dechlorination (Table IV) may indicate that the reductive dehalogenation proceeds via initial formation of the π^* radical anions (Scheme III), which should be more stable than the corresponding σ^* radical anions. Our quantum chemical calculations by using the semiempirical MNDO methodology[45,46] also support this conclusion. The ΔH_f (heat of formation) values of radical anions of PhCl and *p*-CNC_6H_4Cl were calculated by taking the C–Cl bond distance as an independent variable with the rest of geometrical parameters being optimized. The relative energies $[\Delta(\Delta H_f)]$ as compared to those of the standard radical anions at the same C–Cl bond distance as the corresponding neutral molecules are plotted against the bond-stretching distance (ΔC–Cl) as shown in Figure 5, where the energy changes in the π^* and σ^* orbitals with ΔC–Cl are also given. As is clearly seen in the figure there is a sharp energetic barrier in the transition from the π^* to σ^* radicals at the crossing points between the π^* and σ^* orbitals.[47] The higher barrier for

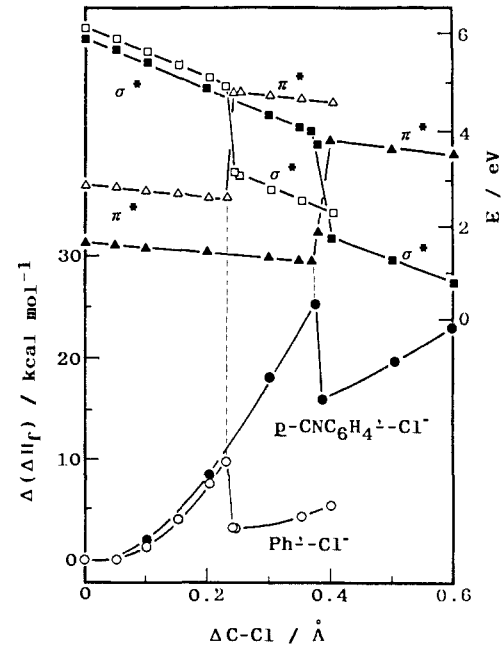

Figure 5. Calculated heat of formation $[\Delta(\Delta H_f)]$ for radical anions of PhCl(○) and *p*-CNC_6H_4Cl(●) relative to ΔH_f at the same C–Cl bond distance as the corresponding neutral molecules and the energies (E) of the respective π^*(△, ▲) and σ^*(□, ■) orbitals plotted against the bond-stretching distance (ΔC–Cl). The MNDO[45,46] calculations of the ΔH_f and E values were carried out by taking the C–Cl bond distance as an independent variable with the rest of geometrical parameters being optimized.

(38) In such a highly exergonic reaction the crossing point between the product and ground-state reactant potential surfaces in the reaction coordinate may appear after the energy minimum of the product potential surface as known as the Marcus inverted region.[39,40] In fact, the relation $\Delta G^{\circ}_{be} < -4\Delta G^{\ddagger}_{0}$ holds in the case of aromatic halides (Tables II and III).

(39) Marcus, R. A.; Sutin, N. *Biochim. Biophys. Acta* **1986**, *811*, 265.

(40) For recent reports on the experimental verification of the Marcus inverted region; see: (a) Fox, L. S.; Kozik, M.; Winkler, J. R.; Gray, H. B. *Science* **1990**, *247*, 1069. (b) Closs, G. L.; Miller, J. R. *Science* **1988**, *240*, 440. (c) Gould, I. R.; Ege, D.; Mattes, S. L.; Farid, S. *J. Am. Chem. Soc.* **1987**, *109*, 3794. (d) DeCosta, D. P.; Pincock, J. A. *J. Am. Chem. Soc.* **1989**, *111*, 8948. (e) Gould, I. R.; Moser, J. E.; Ege, D.; Farid, S. *J. Am. Chem. Soc.* **1988**, *110*, 1991.

(41) In the case of alkyl halides without electron-withdrawing substituents no appreciable energy minimum may exist in the product potential surface, when $\Delta G^{\ddagger}_{br} \simeq \Delta G^{\ddagger}_{be} \simeq 0$.

(42) Moreno, M.; Gallardo, I.; Bertran, J. *J. Chem. Soc., Perkin Trans. 2* **1989**, 2017.

(43) The product ratio was determined under a low conversion condition such that further dehalogenation of primary dehalogenated products can be neglected.

(44) Attachment of slow electrons to *m*-ClC_6H_4Br has been reported to produce more Br^- than Cl^-; see: Naff, W. T.; Compton, R. N.; Cooper, C. D. *J. Chem. Phys.* **1971**, *54*, 212.

(45) (a) Dewar, M. J. S.; Thiel, W. *J. Am. Chem. Soc.* **1977**, *99*, 4899. (b) Dewar, M. J. S.; Thiel, W. *J. Am. Chem. Soc.* **1977**, *99*, 4907.

(46) The personal computer version of a QCPE program by Prof. K. Kitaura (Osaka City University) was used for the calculations.

(47) The energy barrier of the C–Cl bond cleavage in solution may be significantly lower than the calculated value due to the solvation.

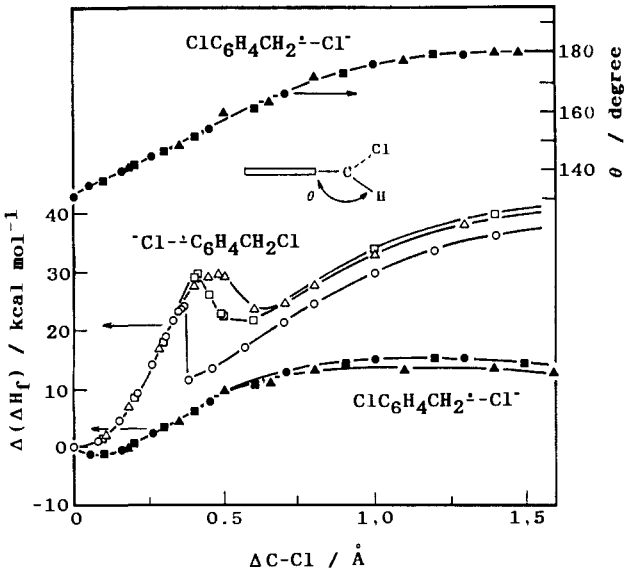

Figure 6. Calculated heat of formation [$\Delta(\Delta H_f)$] for radical anions of *o*-(○, ●), *m*-(△, ▲), and *p*-$ClC_6H_4CH_2Cl$(□, ■) relative to ΔH_f at the same C-Cl bond distance as the corresponding neutral molecules plotted against the bond-stretching distance (ΔC-Cl) of the Cl-C_6H_4 and CH_2-Cl bonds, respectively. The MNDO[45,46] calculations were carried out by taking each C-Cl bond distance as an independent variable with the rest of geometrical parameters being optimized. The geometrical change of the CH_2Cl group with stretching of the CH_2-Cl bond is shown as the plot of the dihedral angle (θ) between the aromatic ring and the CH_2 planes vs ΔC-Cl.

p-$CNC_6H_4Cl^{\bullet-}$ as compared to $PhCl^{\bullet-}$ (Figure 5) agrees with the reported longer lifetime of the former radical anion.[9b]

The more enhanced selectivities are observed in the $AcrH_2$/$AcrH^+$-catalyzed reductive dehalogenation of halobenzyl halides ($X-C_6H_4CH_2X$; X = Cl, Br) with $NaBH_4$ as shown in Table IV, where $X-C_6H_4CH_3$ is obtained selectively with no detectable formation of $PhCH_2X$ in each case. Such highly selective cleavage of the CH_2-X bond as compared to that of the X-C_6H_4 bond may also indicate that the reductive dehalogenation proceeds via initial formation of the π^* radical anions, since the rate of reductive cleavage of the CH_2-X bond would otherwise be comparable with that of the X-C_6H_4 bond, judging from the similar Φ_∞ values of PhX and $PhCH_2X$ (Table III). Figure 6 depicts the energy profiles of the reductive cleavage of both the CH_2-Cl and Cl-C_6H_4 bonds calculated by a similar manner to those in Figure 5, by taking each C-Cl bond distance as an independent variable. As is clearly seen in Figure 6, the energetic barrier in the cleavage of the Cl-C_6H_4 bond is significantly larger than that of the CH_2-Cl bond, in agreement with the observed highly selective cleavage of the CH_2-Cl bond (Table IV). As the CH_2-Cl bond of $ClC_6H_4CH_2Cl^{\bullet-}$ begins to stretch, continuous flattering of $ClC_6H_4CH_2^-$ group occurs to yield $ClC_6H_4CH_2^\bullet$ and Cl^- (Figure 6).

In conclusion, the photocatalytic dehalogenation of aromatic and alkyl halides in the present system may proceed via photoinduced electron transfer from the singlet excited state of 10-methylacridine derivatives used as catalysts to the halogenated compounds, when the bond-breaking process upon the electron transfer can compete well with the back-electron-transfer process to yield the dehalogenated products efficiently. The facile reduction of the oxidized form of 10-methylacridine derivatives with $NaBH_4$ regenerates the catalysts, constituting not only efficient but also stable photocatalytic systems.

Acknowledgment. This work was supported in part by a grant-in-aid (to S. Fukuzumi) for scientific research from Ministry of Education, Science and Culture, Japan. We thank Mr. Y. Tokuda for his single photon counting experiments and Mr. N. Hayashi for his involvement in the early stage of this work.

Specific Asymmetric Fusion between Artificial and Biological Model Membranes

Tino A. A. Fonteyn,[1a] Dick Hoekstra,[1b] and Jan B. F. N. Engberts*,[1a]

Contribution from the Department of Organic Chemistry, University of Groningen, Nijenborgh 16, 9747 AG Groningen, The Netherlands, and Department of Physiological Chemistry, University of Groningen, Bloemsingel 10, 9712 KZ Groningen, The Netherlands. *Received March 23, 1990*

Abstract: Experimental conditions are delineated for specific asymmetric fusion, induced by Ca^{2+} ions, of vesicles formed from di-*n*-dodecyl phosphate (DDP) with phosphatidylserine (PS) and dioleoylphosphatidylcholine (DOPC) liposomes as well as with erythrocyte ghost (EG) membranes. Initial rates and extents of fusion were obtained with the resonance energy transfer assay. The merging of the bilayers rather than vesicle aggregation represents the rate-determining step in the overall fusion event. Unexpectedly, asymmetric PS-DDP and DOPC-DDP vesicle fusion does occur below the main phase-transition temperature of the DDP bilayer. At 25 °C and pH 7.4, DDP vesicles fuse with EG membranes more rapidly and efficiently than PS vesicles. The possible relevance of these findings for cell biological and drug-targetting experiments is pointed out.

Fusion of lipid bilayer membranes is a crucial biological event and occurs, for example, in processes like endo- and exocytosis, cell division, and the infectious entry of viruses into cells.[2,3] Because of the complexities involved in using natural cell membranes, liposomal model systems have been frequently employed to study mechanistic aspects of membrane fusion. Recently we have shown that artificial membrane vesicles formed from simple synthetic surfactants also fuse upon addition of appropriate fusogenic agents and that their fusogenic activity mimics important features of phospholipid membrane fusion.[4] This previous work concerned the occurrence of *symmetric* vesicle fusion, i.e., merging between like vesicle bilayers. Mechanistic studies of the Ca^{2+}-

(1) (a) Department of Organic Chemistry. (b) Department of Physiological Chemistry.
(2) Ohki, S., Doyle, D., Flanagan, T. D., Hui, S. W., Mayhew, E., Eds. *Molecular Mechanisms of Membrane Fusion*; Plenum: New York, 1988.
(3) Hoekstra, D.; Kok, J. W. *Biosci. Rep.* **1989**, *9*, 273.
(4) (a) Rupert, L. A. M.; Hoekstra, D.; Engberts, J. B. F. N. *J. Am. Chem. Soc.* **1985**, *107*, 2628. (b) Rupert, L. A. M.; Engberts, J. B. F. N.; Hoekstra, D. *J. Am. Chem. Soc.* **1986**, *108*, 3920. (c) Rupert, L. A. M.; Van Breemen, J. F. L.; Van Bruggen, E. F. J.; Engberts, J. B. F. N.; Hoekstra, D. *J. Membr. Biol.* **1987**, *95*, 255. (d) Rupert, L. A. M.; Hoekstra, D.; Engberts, J. B. F. N. *J. Colloid Interface Sci.* **1987**, *120*, 125. (e) Rupert, L. A. M.; Van Breemen, J. F. L.; Hoekstra, D.; Engberts, J. B. F. N. *J. Phys. Chem.* **1988**, *92*, 4416. (f) Rupert, L. A. M.; Hoekstra, D.; Engberts, J. B. F. N. *J. Colloid Interface Sci.* **1989**, *130*, 271.

0002-7863/90/1512-8870$02.50/0